Visualization of Activity Data from a Sensor-based Long-Term Monitoring Study at a Playground

Tobias Bolten[1], Regina Pohle-Fröhlich[1], Dorothee Volker[2], Clemens Brück[2], Nicolas Beucker[2] and Hans-Günter Hirsch[1]

[1] *Institute of Pattern Recognition, Niederrhein University of Applied Sciences, Reinarzstr. 49, Krefeld, Germany*

[2] *Competence Center for Social Urban Design, Niederrhein University of Applied Sciences, Frankenring 20, Krefeld, Germany*

{*tobias.bolten, regina.pohle, dorothee.volker, clemens.brueck, nicolas.beucker, hans-guenter.hirsch*}*@hs-niederrhein.de*

Keywords: Activity Visualization, Heat map, Long-Term Monitoring, Dynamic Vision Sensor

Abstract: In the context of urban planning, a detailed knowledge of the considered space and its utilization is essential. However, manual observations are often not performed due to cost. Whereas sensor-based systems are often not installed due to possible constrains caused by data protection laws and user privacy-concerns. We addressed these concerns and developed a privacy-aware, sensor-based processing pipeline for detecting objects based on an analysis of signals from several sensors. These detections are used for their mapping and visualization in a global bird eye view.

Besides a data normalization, which is crucial considering sections of different lengths, multiple variations of activity visualization applying heat maps are described. This includes the utilization of background representations with different levels of details, different accumulations of object detections through the adjustment of the performed spatial binning as well as applying different colormaps. Both sequential colormaps and diverging colormaps with and without perceptually uniform distances were considered.

These variations were evaluated in a conducted online survey addressing professional urban planners as well as interested citizens. The results of this survey were used to determine a meaningful default setup for visualizing the activities in an interactive graphical user interface. This interface is intended to make the results of the performed long-term monitoring generally accessible.

1 INTRODUCTION

In order to realize an user-oriented perspective for planning and designing public spaces, urban planners need detailed knowledge about the future or current users of an urban space. For this reason, a long-term observation of the behavior of the different user groups in the public space is necessary.

Until now the analysis of interaction in public space is generally still based on analogue methods, which leads to rather expensive user studies. Manual methods are mainly preferred because of ethical standards concerning pattern recognition and the surplus of ad hoc interpretation by professional observers (Gehl and Svarre, 2013). Depending on very different international legislations, monitoring by means of classic CCTV systems is often associated with high regulatory requirements. Regardless of the legal constraints, these CCTV systems can also be associated with user concerns regarding data protection aspects.

In this paper, we present generated activity visualizations resulting from a sensor-based long-term study conducted in a living lab context of a public children's playground. Within this study, the aforementioned user concerns were considered and addressed through an alternative, privacy-compliant sensor selection. The goal is to use these evidence-based activity observations as a resource to evaluate spatial use and optimize urban design considerations.

Due to the long-term aspect of this monitoring and the utilization of multiple sensors, a large amount of data is generated in this process. Therefore, it is necessary to visualize it in a suitable manner. The key is a presentation in a way that decision makers can understand and interpret the diverse collected information. For this purpose, we are examining several aspects of activity visualization and investigate them using examples through a conducted user study among professional decision makers in the urban planning environment. Furthermore we are exploring the visualization of various data based insights in one interface in order to generate a user friendly overview of complex situations.

The paper is structured as follows. Section 2 summarizes related work in the context of activity visualization. A detailed description of the monitored area and the processing pipeline used for activity detection follows in Section 3. In Section 4 the investigated visualizations, as well as their creation is described. First results of the user study are summarized in Section 5. Finally, an overall summary and outlook for an integrated user friendly interface is provided in Section 6.

2 RELATED WORK

There are different approaches for the visualization of space-time data in the literature. For example, measured parameters can be used to color individual objects of the observed infrastructure. However, the observed playground in this study is designed as a nature experience space and therefore does not contain classic playground equipment, but rather different areas in which the children can playfully interact with natural materials. Therefore, in this practical case, playground equipment representations cannot be used for visualization.

More popular is the visualization of the measured values from the user's perspective by creating usage maps. It can be observed that abstract 2D representations are preferred compared to 3D representations. This is certainly also due to the fact that 2D representations do not require any additional interaction when interpreting the data. In some projects, such as (Rezaei and Azarmi, 2020), both options are used to visualize tracking and distance maps.

In addition to conveying the acquired data by means of coloring as 2D or 3D heat map, there are also many examples on the web that use simple shapes such as circles, spheres, or cubes to represent site-specific information (Geospatial, 2021). Depending on the type of available data and the desired type of information to be conveyed, human movements in public spaces are visualized in different ways. For example, to visualize the paths of individual visitors, Cuellar chooses a single flow representation (Cuellar et al., 2020), while Laureyssens chooses non-personalized flow maps (Lauressens, 2005) to display pedestrian lanes in a public square. In the flow map in (Nielsen et al., 2014), it is possible to assign the flow lines to individual moving people. An extension of flow maps can be found in (Peysakhovich and Hurter, 2017). Here, in addition to the path of the movement, the direction of the movement is also used in a flow direction map to display the results of eye tracking.

Scatterplots are used to visualize fewer recorded events at a location, such as showing manually counted people in a street segment within a limited time period. This is for example described by Whyte in (Whyte, 1979), who was a pioneer of systematic user analysis in urban planning. Very often, heat maps can also be found to represent captured people when automatic data collection is performed, e.g., in (Rajasekaran et al., 2020) to represent group activities in student dormitories. In (Rashed et al., 2016) heat maps are used to analyze which exhibit in a museum is particularly popular for visitors. Bolleter also uses heat maps to present his results of Wi-Fi tracking in public spaces to count people and map their stays and movements at the district level (Bolleter, 2017).

When using heat maps, it should be noted that the selection of an appropriate color table and a scaling adapted to the problem are crucial for the subsequent interpretation of the data (Eghteabs et al., 2017). In addition, when selecting the color tables, it is important to consider that color-blind people can also interpret the data and that older people are less sensitive to colors (Silva et al., 2011).

Different types of generation for colormaps are described in the literature (Zhou and Hansen, 2015). Colormaps can be generated procedurally, with the goal of being able to interact with as many different data sets as possible. For some tasks, user studies exist that were used to develop suitable colormaps. Furthermore, perception-based rules learned in the course of life exist for certain applications. An example of this is the communication of the measured temperature via a blue-red scale. For our monitoring application, the data-driven generation is relevant to make both, the short-time and the long-term data, interpretable in a similar way with an adapted colormap. For visualization of such ordinal data, sequential perceptually uniform maps should be used that reflect numerically equal distances between values for equally perceived color differences (Moreland, 2009).

3 DATA ACQUISITION AND PROCESSING

This section presents the developed processing chain from the activity recording performed by multiple sensors to the derived coordinates for a joint visualization.

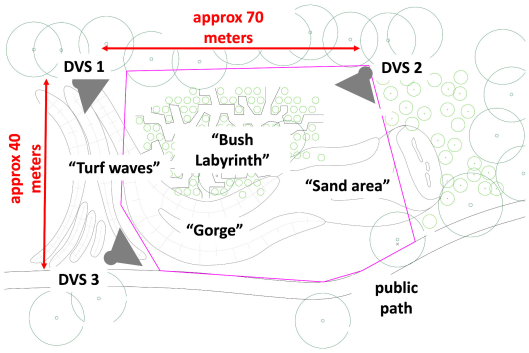

Figure 1: Schematic plan of the measuring area and sensor positioning (adapted from (Bolten et al., 2021b)).

3.1 Living Lab

The schematic plan of the children's playground, which serves as a study area within the living lab, is shown in Figure 1. This area has an approximate size of 2800 square meters and is covered by three permanently mounted sensors. The recording scenario of this long-time observation corresponds to the technical setup of (Bolten et al., 2021b) and can be summarized and quoted as follows.

Each of the sensors is mounted on a pole at a height of approximately 6 meters with an angle of inclination of approximately 25 degrees to the ground. The positioning of the sensors was chosen in such a way that blind spots created by the terrain (trees, bushes, hills) are minimized as far as possible. Furthermore, it was tried to cover all areas by more than one sensor. The recording period of each sensor covered the timespan from 10am to 8pm a day all week, which results in a very large amount of data that serves as a basis for visualization.

3.2 Privacy-aware Activity Data Collection

Activity on the playground was captured using three CeleX4 Dynamic Vision Sensors (DVS) (Guo et al., 2017), each equipped with a 8mm wide-angle lens. Compared to conventional cameras, these sensors do not record intensity frames, but capture only changes in brightness as a sparse stream of so called events. Each pixel of a DVS operates independently and asynchronously from each other and triggers an output event when a brightness change above a threshold has been detected. An event $e = \{(x,y),t,p\}$ contains only the spatial position (x,y) of the triggered pixel, a timestamp t and the polarity p of the brightness change.

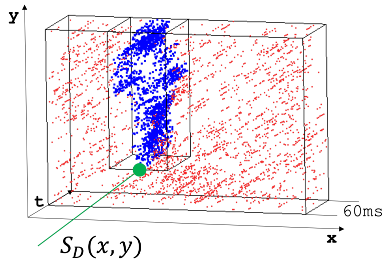

Figure 2: Semantic segmentation result of DVS event stream with derived object detection coordinate $S_D(x,y)$

These types of vision sensors offer a fundamental advantage in terms of data privacy aspects, as no gray or color values need to be processed in any software logic to evaluate the activity within the scene. These inherent hardware-based sensor characteristics allow DVS technology to be used under significantly lower legal data protection requirements compared to traditional CCTV systems. Furthermore, the DVS technology also offers reduced data redundancy through the data-driven output paradigm of the sensor, as well as a higher dynamic range, lower power consumption and higher temporal resolution compared to classic CCD/CMOS imagers. The utilized CeleX4 sensor offers a spatial resolution of 768×640 pixels, of which 768×512 pixels are effectively used due to technical limitations.

To analyze the event stream, an event-wise semantic segmentation is carried out for contiguous temporal windows of the data streams, each of 60ms duration. This segmentation is achieved by applying a PointNet++(Qi et al., 2017) deep neuronal network structure, which is especially designed for the processing of unordered point clouds. Thus, each event is assigned a label out of a set of 10 classes in total. In addition to the classes person, dog, bicycle and sportsball, which represented objects of interest in the performed monitoring, six classes for environmental influences, such as bird, insect, tree crown, tree shadow, rain, and shadows were considered. This segmentation step is based on (Bolten et al., 2021a) and their published models. According to the evaluation provided in this paper, the PointNet++ processing achieves an occurrence frequency weighted F1-score of $\approx 93\%$ over all mentioned classes on the DVS-OUTLAB dataset (Bolten et al., 2021b), which was recorded in the same application context as this work.

Within the segmented event stream, the events of classes of interest are clustered and thereby the detection coordinates $S_D(x,y)$ relative to field of view from sensor S are determined. As an example, a detected person is shown in Figure 2.

In addition to the data collected with the DVS, weather data was also recorded to be included in the

(a) 3D Rendering (b) Wireframe

Figure 3: Calculated SFM 3D model of the playground

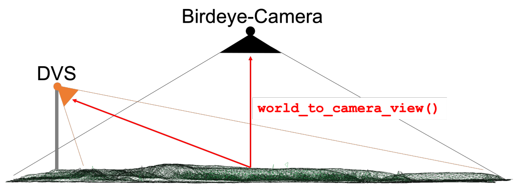

Figure 4: 3D model based coordinate lookup table generation

planned interface as illustrated in Figures 13. This data can contribute to a better estimation of the use of the play area at a certain time, as fewer users can be expected during cool rainy weather than during warm sunny weather.

3.3 3D Model-based Bird's Eye View Mapping

The next step within the processing pipeline used for visualization is to map the object detections $S_D(x,y)$, which are relative to the sensor field of view, into a global representation such as a top or blueprint view like Figure 1.

The mapping of these object detection coordinates is not a trivial task due to the heavy terrain modeling (like hills and valleys) of the monitored playground area. Due to these terrain properties, a simple affine transformation between the sensor field of view and the map representation leads to very large inaccuracies, since no flat surface plane is given.

To achieve a more accurate estimate, we calculated a 3D model of the playground area, and performing the mapping based on this model. In this way, the terrain modeling is included in the applied transformation. This 3D model was generated using 285 images from a drone overflight. In these overlapping images, the camera positions are estimated based on determined corresponding points using structure from motion (SFM) technique. Based on these camera positions, the 3D points of the model are calculated. We used the commercial software AgiSoft[1] for this purpose. A 3D rendering of the created model is shown in Figure 3a, where Figure 3b highlights the included terrain characteristics of the model.

[1] https://www.agisoft.com/

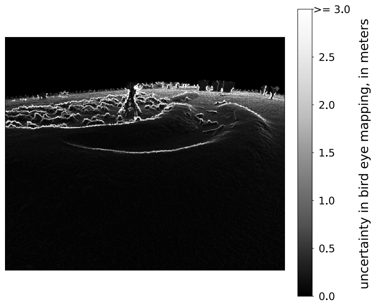

Figure 5: Uncertainty visualization of performed $S_D(x,y)$ to $B_D(x',y')$ point mapping, exemplary for one sensor

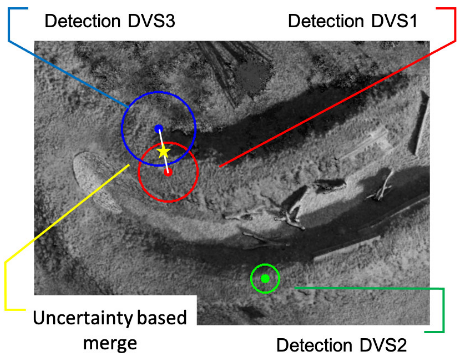

Figure 6: Cropped and zoomed example of uncertainty based merging of projected bird eye detections

Afterwards the calculated 3D model of the playground is used in a 3D simulation created with Blender[2]. Within this simulation, camera objects were positioned and aligned with the same parameters as the used DVS sensors (such as sensor size, resolution, focal length). In addition, a bird eye camera B was positioned. Through this simulation, the relation of the 3D model mesh vertices to the respective pixel coordinates in the DVS view or bird eye view can be determined. In this way, a lookup table was generated that allows a mapping from $S_D(x,y)$ to $B_D(x',y')$ within the rendered top view. This processing is illustrated in Figure 4.

3.4 Fusion of Detections from Multiple Sensors

The described method achieves a high quality mapping between the (x,y) coordinates in the sensor view to corresponding points in the bird eye top view. However, due to the terrain modeling, there are still leaps in this bird eye view mapping. Figure 5 shows this as an example for one of the sensors. Here the maximum distance in the bird eye projection is shown for each point $S_D(x,y)$ of the sensor view, which re-

[2] https://www.blender.org/

sults when projecting the coordinates within the 8-connected neighborhood $S_D(x \pm 1, y \pm 1)$ around this point. On the ridges of the terrain modeling projection distances of several meters can result by shifting the sensor detection by only one pixel. This distance is taken into account as an "uncertainty factor" when merging the detections from all sensors into a joint representation.

For temporal synchronous detections from different sensors, it is tested whether there are overlaps to other detections within these uncertainty distances. This procedure is illustrated in Figure 6. In this example, the filled circles correspond to synchronous detections from the sensors and the outer circles indicate the corresponding uncertainty distances of the bird mapping. The radii of the detections of DVS1 and DVS3 overlap in this case and are therefore combined into one detection.

4 STUDIED VISUALIZATIONS

In the following, the accumulation logic for a consolidated visualization of the merged object detections is presented. This includes data binning as well as normalization. Subsequently, different generated and studied visualizations variants are presented. All generated activity plots were created using the `matplotlib` library(Hunter, 2007).

4.1 Spatial- and Temporal Detection Binning

In order to visualize the activity level on the playground area, the bird eye view is divided into several sub-areas in the form of a spatial binning. For each subarea, the activity is then determined and plotted. The grid for this spatial partitioning is approximately 0.5 to 1 square meter per bin. This selection was made in order to be able to identify slight location differences in the usage-frequency despite the overall size of the monitored area.

Within the performed long-term observations, there are periods of very different lengths in which an activity has taken place on the site. Since both short-time and long-term aspects are of interest within the evaluation, the ability to visualize time intervals of different lengths is essential. This results in the challenge that the displayed activity levels (low to high) must be comparable with each other when visualizing periods of different lengths by using the same color values. For this reason, we apply the following normalization technique.

In addition to the described spatial binning of the observed area, a further temporal binning is performed. For each spatial bin, the detections of that area are sorted temporally. The complete temporal interval considered for visualization is then divided into smaller sections and the count of these smaller temporal sections containing at least one object detection is determined. In this way, a percentage normalization between $[0, 1]$ is realized as a function of the considered total duration.

For example, a considered observation time for visualization of one hour and a division into temporal bins of one minute length results in a scaling of $x/60$, with x being the number of populated one minute detection time blocks. The division into these short time segments (e.g. one minute) is possible because the semantic analysis of the DVS event stream is performed in much shorter time windows of only 60ms duration, as explained in Section 3.2.

4.2 Considered Heat-Map Variations

Then the merged, binned and normalized object detection data is visualized in the form of heat maps to give decision-makers an intuitive and quick overview and to make significant areas of usage easily recognizable.

Different variations in the generation of these heat maps were considered and evaluated:

Level of detail in bird eye view (LoD)
: For a spatial orientation of the visualized activity detections, a representation of the monitored area is crucial. However, the background image used as site representation can be carried out in different levels of detail.

: Photorealistic rendered variants from the created 3D Blender model simulation, as well as further abstracted sketches of the considered area were evaluated in our work. Examples of these background image variants in color, as well as in grayscale, are shown in Figure 7.

2D vs 3D display dimensionality
: Display variants with a 2-dimensional and a 3-dimensional rendering of the plot were created.

: In the case of the 3D display, the activity is represented by the height of a three-dimensional surface in addition to the used color. An example of this is given in Figure 8a. Since a change of the viewport is necessary to interpret these 3D views, animations were created containing a 360 degree rotation of the plot.

: A representation as a two-dimensional image, on the other hand, allows the data to be interpreted

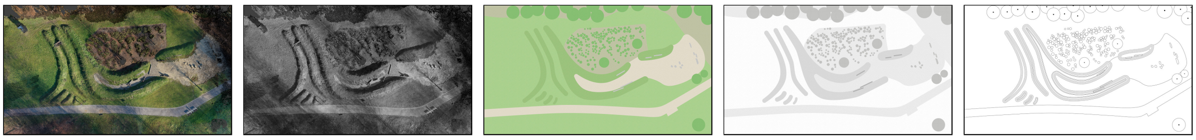

(a) RGB Rendering (b) Greyscale rendering (c) RGB sketch (d) Greyscale sketch (e) Simplified sketch

Figure 7: Used level of detail in bird eye view

(a) 3D with animated viewport (b) 2D projection

Figure 8: Spatial display variants in 2D and 3D

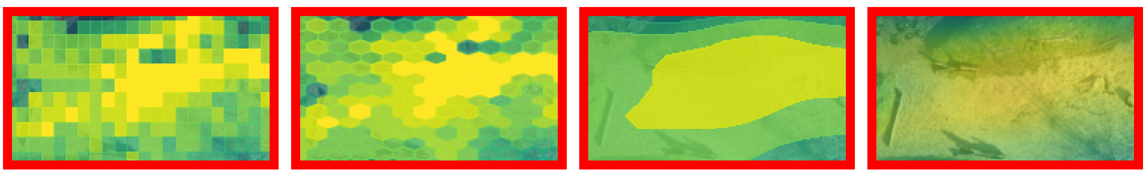

(a) Rectangles (b) Hexagons (c) Contour (d) Continuous density, resulting from KDE

Figure 9: Applied spatial binning and display variants (highlighted region from Figure 8b)

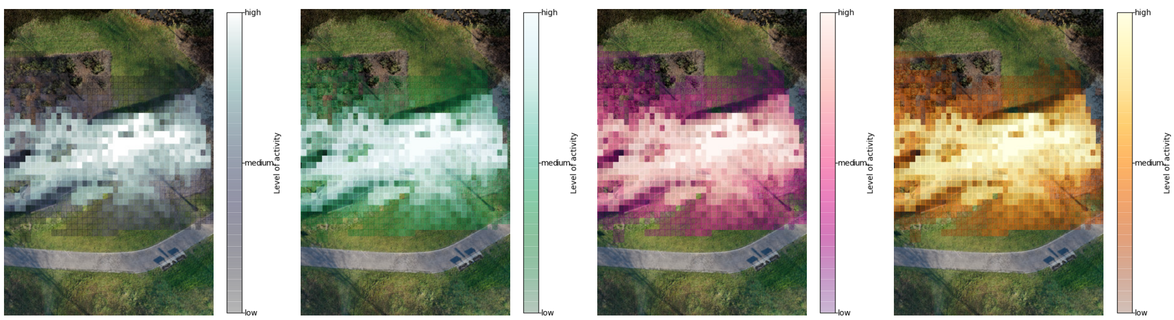

(a) Bone (b) BuGn (c) RdPu (d) YlOrBr

Figure 10: Applied sequential colormaps

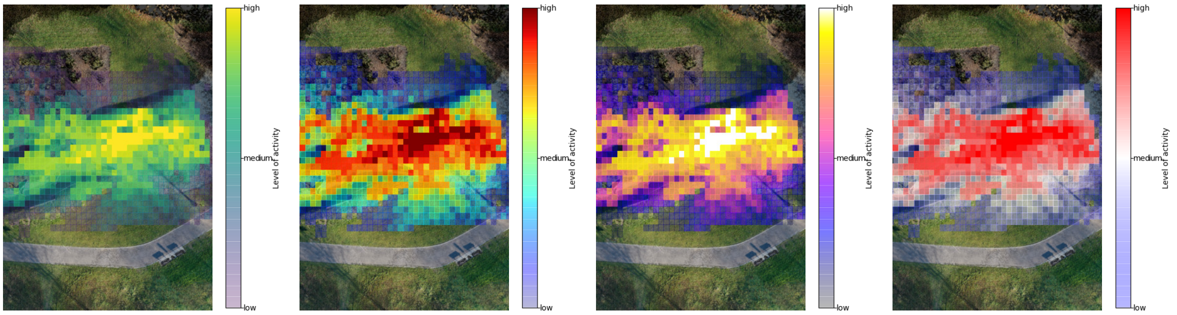

(a) Viridis (b) Jet (c) Gnuplot2 (d) Bwr

Figure 11: Applied diverging colormaps

without this type of animation or interaction. A corresponding example for this visualization is given in Figure 8b.

Spatial binning variants

Besides the straightforward variant of the spatial (x,y)-binning into rectangular tiles we also applied a tessellation by regular hexagons, as displayed in Figures 9a and 9b. In addition, a contour-based representation was implemented, which shows areas with approximately similar usage appropriately grouped together (Figure 9c).

The variants mentioned so far have a discontinuity of the generated representation in common. To provide an alternative for this, a Kernel-Density-Estimation (KDE) based variant was also created, which allows a gradually smooth representation of the activity level. An example of this is given in Figure 9d.

Colormap variations

Compared to long-learned and daily applied colormaps (e.g. in weather forecasts), the question is which colormap is best suitable, interpretable and to intuitively associated with a level of activity by the addressed decision makers.

For this purpose, various simple sequential colormaps (Figure 10), as well as further diverging colormaps (Figure 11) were examined. In case of the diverging colormaps, contrary to usual use-cases, the common application of a center-point within the double-ended color gradient was omitted. This results in a continuous color fading of the normalized activity level from low to high through this center point.

Perceptually uniform perceived colormaps were also taken into account in this colormap consideration. In addition the direction of the used colormap to encode the activity level, i.e. from dark to bright or vice versa, were also considered.

A linear alpha-blending with higher transparency factors for lower activity levels was used within the colormap to overlay the generated activity visualizations over the selected plot background image.

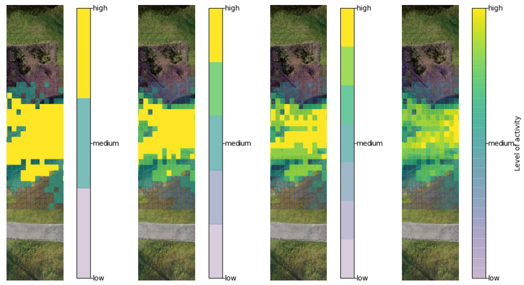

(a) 3 (b) 5 (c) 7 (d) 255

Figure 12: Used level of detail in activity colormap through further binning it into n blocks

5 USER STUDY

The previously described representations of the activity heat maps were evaluated in an online survey. The carefully selected participants came from professional backgrounds in urban planning and interaction design, but also interested citizens were involved in order to reflect the laymans perspective. The survey was designed to check the comprehensibility of the generated activity representations by heat maps, which were created based on design assumptions regarding readability and experiential knowledge, and to identify adequate default settings for upcoming visualizations and applications. Sixteen participants took part in the online survey. They had the opportunity to rate the different visualizations and were asked to comment their decisions.

The results show trends and confirm previously made assumptions. Table 1 summarizes numerically the survey results described below.

5.1 Visualization of the Playground

The RGB rendering of the bird eye image (Figure 7a) was selected as the preferred variant. But the comments revealed that the displayed user activity could not be related precisely as the heat maps covered the image with solid colors.

Regarding the 3D rendering, it can be stated that a high user activity is displayed with a large distance from the map, which makes the assignment more difficult.

5.2 Colormaps and Binning

In terms of color, it can be summarized that color maps with diverging colors are preferentially associated with user activity. One assumption why these diverging colormaps were preferred over the sequential ones is that they offer a higher contrast and are thus, also for older users, more clearly distinguishable. This contrast discrepancy is further enhanced by the amplified alpha blending factor used at lower activity levels (compare to Section 4.2).

However, contrary to the widespread assumption from the literature (Moreland, 2009), no perceptually uniform colormap was preferred. The color map `jet` (Figure 11b) was preferred by the participants. We assume that this color map preference indirectly draws on experiential knowledge (weather representation, from blue to red), leading to a corresponding association and increased intelligibility.

For the spatial binnings, the representation of user activity in rectangles was selected by most of the respondents (Figure 9a). This preference matches with established representations. Similar rectangular grids were already used by the pioneer of spatial observations William H. Whyte who investigated human behavior in urban environments in the early 1970s. Whyte was the first researcher using a video camera for long term spatial observations. His study protocols are still leading information graphics in the field of urban studies (Whyte, 1980).

Regarding the applied colormaps a further simplification was evaluated within the user survey. This approach consists of quantizing the continuous activity scale into coarser sections, as illustrated in Figure 12. The idea here was to clearly divide the activity into referenceable blocks from “low” to “high”. However, the participants of the study clearly preferred the full color gradient with 255 colors (compare to Figure 12d). Therefore, a division of the color scale has not been considered further, since this also goes ahead with a loss of information and makes it more difficult to identify hotspots on the plot.

5.3 Plausibility and Implemented Changes

In the online survey, the plausibility was checked last. The users were shown a map with three marked areas. They were asked to select in which marked area the highest user activity was measured. 15 out of 16 people chose the correct answer. This confirms the comprehensibility of the presentation as well as the presentation in the top view.

With the results from the survey, the visualization was adjusted, and the sketch-drawing of the playground was placed as an overlay on the rendering and the user activity (compare with heat map in Figure 13). This allows the exact assignment of the user activity.

6 CONCLUSION

In the conducted research we successfully explored methods of collecting anonymized data that allow the tracing of spatial use. The studied visualizations offer a basis for the design of an integrated interface that can be used by urban planners to evaluate the interaction within a determined area. The project aims to collect open data in the terms of the Smart City to inform stakeholders and thus to provide an objective basis for discussion of decisions and changes. The complex results are to be made available to urban planners and interested citizens in an interactive interface.

This interface, an example is given in Figure 13, will give the opportunity to select individual time frames, spatial focus and further details of weather conditions and other measurements that are easily available and give insights about the circumstances during the use of the site.

Outlook

In the current visualizations, only the measured activity level of a single class (PERSON in the examples shown in this work) is considered and displayed. Therefore, one aspect for further work is the evaluation of methods for a consolidated visualization of activity caused by a set of multiple classes. One goal here would be to allow a further differentiation of the underlying activity levels per class. This could be achieved through the interactive usage of different visualization layers or the integration of spatial icons in this activity visualization.

A second step in the further development would be the improvement of the sensor signal processing pipeline to achieve a continuous object tracking instead of a semantic segmentation. This leads to the question of how a long-term aggregated representation of these directed object movements should be visualized. These aspects should also be evaluated subsequently in the form of another user-study.

ACKNOWLEDGEMENTS

We thank Felix Lentzen for his technical support and work related to the described Blender based bird eye view mapping.

Funding

This work was supported by the European Regional Development Fund under grant number EFRE-0801082 as part of the project "plsm" (https://plsm-project.com/).

REFERENCES

Bolleter, J. (2017). Counter intelligence: evaluating wifi tracking data for augmenting conventional public space–public life surveys. *Australian Planner*, 54(2):134–144.

Bolten, T., Lentzen, F., Pohle-Fröhlich, R., and Tönnies, K. D. (2021a). Evaluation of deep learning based 3d-point-cloud processing techniques for semantic segmentation of neuromorphic vision sensor event-streams. *arXiv*.

Bolten, T., Pohle-Fröhlich, R., and Tönnies, K. D. (2021b). Dvs-outlab: A neuromorphic event-based long time monitoring dataset for real-world outdoor scenarios. In *Proceedings of the IEEE/CVF Conference on Computer Vision and Pattern Recognition (CVPR) Workshops*, pages 1348–1357.

Cuellar, K., Jambor, E., Sorornejad, P., and Talpey, S. (2020). Improving visitor evaluation at the british museum. Worcester Polytechnic Institute.

Eghteabs, C., Ritter, B., Parikh, A., and Lischke, L. (2017). Effects of color and threshold on user perception of heat maps. In *Proceedings of the 2017 ACM Conference Companion Publication on Designing Interactive Systems*, pages 275–279.

Gehl, J. and Svarre, B. (2013). *How to Study Public Life*. Island Press, Washington, Covelo, London.

Geospatial, C. T. P. D. (2021). Use cases. https://cesium.com/use-cases/. Online; accessed 2021-08-20.

Guo, M., Huang, J., and Chen, S. (2017). Live demonstration: A 768 x 640 pixels 200meps dynamic vision sensor. *2017 IEEE International Symposium on Circuits and Systems (ISCAS)*, page 1.

Hunter, J. D. (2007). Matplotlib: A 2d graphics environment. *Computing in Science & Engineering*, 9(3):90–95.

Lauressens, T. (2005). Pedestrian levitation.net. http://www.visualcomplexity.com/vc/project.cfm?id=255. Online; accessed 2021-08-20.

Moreland, K. (2009). Diverging color maps for scientific visualization. In *International Symposium on Visual Computing*, pages 92–103. Springer.

Nielsen, S. Z., Gade, R., Moeslund, T. B., and Skov-Petersen, H. (2014). Measuring human movement patterns and behaviors in public spaces. a method based on thermal cameras, computer vision, and geographical information system technologies. *Measuring Behavior 2014*.

Peysakhovich, V. and Hurter, C. (2017). Scanpath visualization and comparison using visual aggregation techniques. *Journal of Eye Movement Research*, 10(5).

Qi, C. R., Yi, L., Su, H., and Guibas, L. J. (2017). Pointnet++: Deep hierarchical feature learning on point sets in a metric space. In *Proceedings of the 31st International Conference on Neural Information Processing Systems*, NIPS'17, pages 5105–5114, Red Hook, NY, USA. Curran Associates Inc.

Rajasekaran, R., Rasool, F., Srivastava, S., Masih, J., and Rajest, S. S. (2020). Heat maps for human group activity in academic blocks. In *Business Intelligence for Enterprise Internet of Things*, pages 241–251. Springer.

Rashed, M. G., Suzuki, R., Yonezawa, T., Lam, A., Kobayashi, Y., and Kuno, Y. (2016). Tracking visitors in a real museum for behavioral analysis. In *2016 Joint 8th International Conference on Soft Computing and Intelligent Systems (SCIS) and 17th International Symposium on Advanced Intelligent Systems (ISIS)*, pages 80–85. IEEE.

Rezaei, M. and Azarmi, M. (2020). Deepsocial: Social distancing monitoring and infection risk assessment in covid-19 pandemic. *Applied Sciences*, 10(21):7514.

Silva, S., Santos, B. S., and Madeira, J. (2011). Using color in visualization: A survey. *Computers & Graphics*, 35(2):320–333.

Whyte, W. H. (1979). New york and tokyo: A study in crowding. *Real Estate Issues*, 4(2):117.

Whyte, W. H. (1980). *The social life of small urban spaces*. Conservation Foundation, Washington, D.C.

Zhou, L. and Hansen, C. D. (2015). A survey of colormaps in visualization. *IEEE transactions on visualization and computer graphics*, 22(8):2051–2069.

Aspect of question	Options					
	RGB Rendering	Grey Rendering	RGB Sketch	Grey Sketch	Simpl. Sketch	None
LoD Bird eye view (Fig. 7)	**9**	0	1	2	3	1
	3D animated	**2D RGB**	2D Grey	2D RGB Sketch	2D Grey Sketch	2D Simpl. Sketch
3D / 2D representation (Fig. 8)	0	**9**	1	1	4	1
	Rectangles	Hexagons	Contour	KDE		
Spatial binning (Fig. 9)	**7**	1	3	5		
	Bone	**BuGn**	RdPu	YlOrBr	None	
Sequential colormaps (Fig. 10)	3	**5**	4	2	2	
	Viridis	**Jet**	Gnuplot2	Bwr		
Diverging colormaps (Fig. 11)	2	**9**	3	2		
	3 Blocks	5 Blocks	7 Blocks	**Full**		
Colormap binning (Fig. 12)	2	0	4	**10**		

Table 1: Summarized overview of response rates of the user survey

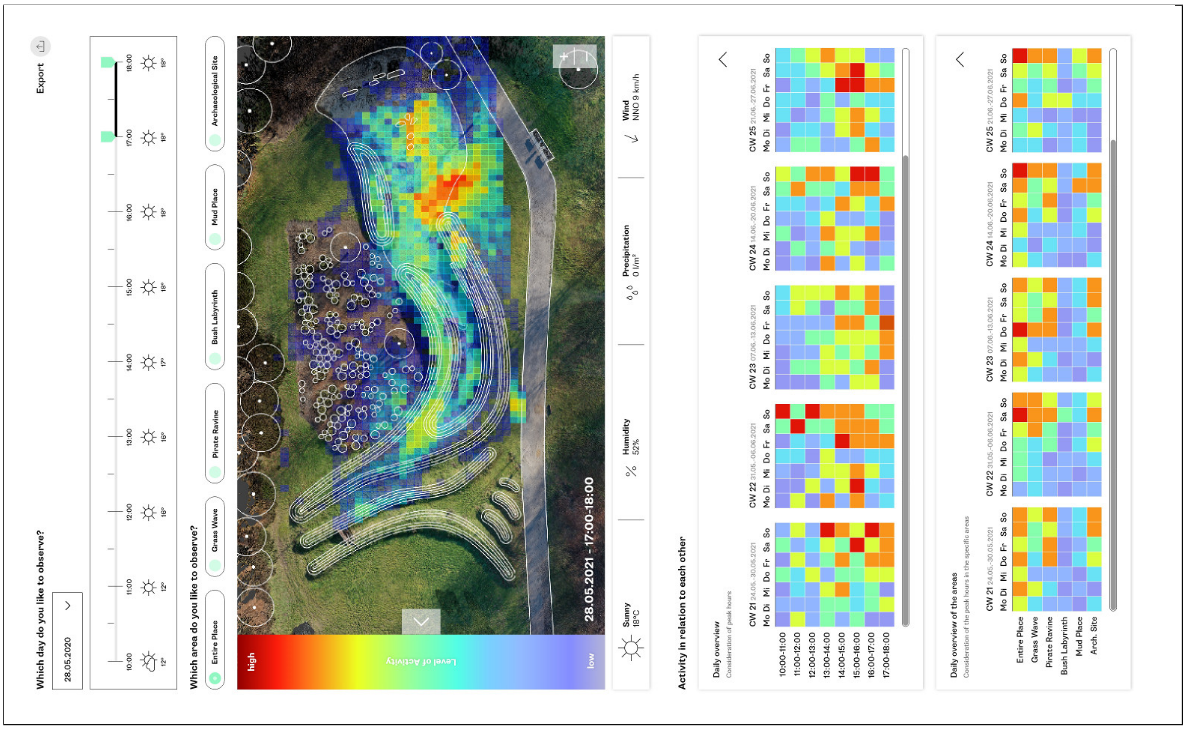

Figure 13: Example for prototyped user-interface